Research Square

Preprints are preliminary reports that have not undergone peer review.
They should not be considered conclusive, used to inform clinical practice,
or referenced by the media as validated information.

Diversification of the Corophiida amphipod silk-spinning systems

Siena McKim

smckim@ucsb.edu

University of California, Santa Barbara

Brittany Cummings

Florida Museum of Natural History

Siena Waldman

University of California, Santa Barbara

Antonia Johnstone

The University of Western Australia

Adam Wall

Natural History Museum of Los Angeles County

Kevin Kocot

University of Alabama

Thomas Turner

University of California, Santa Barbara

Research Article

Keywords:

Posted Date: July 1st, 2026

DOI: https://doi.org/10.21203/rs.3.rs-10085165/v1

License: This work is licensed under a Creative Commons Attribution 4.0 International License.
Read Full License

Additional Declarations: No competing interests reported.

Diversification of the Corophiida amphipod silk-spinning systems

Siena McKim, Brittany Cummings, Siena Waldman, Antonia Johnstone, Adam Wall, Kevin Kocot, & Thomas Turner

Abstract

Silk has evolved independently at least 30 times across arthropods, yet nearly all research on silk evolution has focused on insects and spiders. As a result, we know remarkably little about how silk-spinning systems originated and diversified in other arthropod lineages. Corophiidan amphipods (Amphipoda: Corophiida) are a morphologically and ecologically diverse group of marine crustaceans that produce silk for tube and domicile construction, substrate attachment, and food capture, but no extensive comparative study has examined the morphology or evolution of their silk-spinning systems. Here, we present the largest morphological survey of corophiidan silk-spinning systems to date, examining 40 species and investigating silk-spinning system evolution through ancestral state reconstruction and correlated trait evolution analyses. We confirm a conserved organizational framework ancestral to corophiidans, comprising two pseudotubular gland types and a shared dactylar silk-extrusion morphology. We also document substantial underdescribed morphological diversity of structures that transform silk prior to extrusion. Modified reservoir chambers and the production of strong attachment silk co-evolved in a strictly correlated and irreversible manner, arising independently at least four times through distinct structural solutions. In lineages that do not construct domiciles, like the Podoceridae, we demonstrate that silk-spinning morphology is retained but the function is unknown. This highlights the need to decouple silk-spinning capacity from domicile-building behavior. These findings establish corophiidan amphipods as a compelling system for investigating the evolution of silk, with broader implications for biomaterials research and our understanding of how silk-spinning systems diversify.

Introduction

Silk is among the most important evolutionary innovations in arthropods. It has evolved independently at least 30 times and is used by hundreds of thousands of species for feeding, protection, and social and reproductive behaviors (Craig, 1997; Sutherland *et al*., 2010; Robson *et al*., 2015; Reboleira & Enghoff, 2016). Across arachnids and insects, silk-spinning systems and the silks they produce are adapted to diverse ecological challenges, and evidence for their repeated origins is reflected in the remarkable diversity of spinning morphologies found across the arthropod tree of life (Sutherland *et al.*, 2012; Craig 1997). Several crustacean groups are also known to produce silk, including isopods (Gorvett 1952), tanaids (Kakui *et al.*, 2021), and amphipods (Kronenberger *et al.*, 2012a; Neretin, 2016; Neretin *et al*., 2017; McKim & Turner, 2024). Within amphipods, silk-spinning has evolved independently at least twice, in Ampeliscidae and Corophiida (Schellenberg, 1925; McKim & Turner, 2024; McKim & Turner, *in review*). Among these lineages, corophiidan amphipods exhibit exceptional diversity in both silk architecture and silk use.

Corophiidans use silk to construct a wide variety of structures (Myers & Lowry, 2003). Species build silk-based tubes, domiciles, and rods within diverse habitats which are used for suspension feeding, shelter, and rearing young (Shillaker & Moore, 1978; Shillaker & Moore, 1987; Dixon & Moore, 1997; Cerda *et a*l., 2010; Neretin *et al*., 2017). Silk architecture and composition vary considerably across lineages. For example, species in the families Corophiidae and Aoroidae assemble fragile tubes in sediment and on algae from a homogeneous silk (Shillaker & Moore, 1978; Dixon & Moore, 1997). In contrast, species in the families Photidae, Amphithoidae, and Dulichiidae produce complex structures composed of multiple silk types with strong attachment threads anchoring the structures to the substrate (Fig. 1) (Skutch, 1926; Carter, 1982; Neretin, 2016; Neretin *et al.*, 2017).

This diversity extends beyond silk structures themselves to the morphology of the silk-spinning systems that produce them. Although canonical silk is produced in insects, arachnids, and crustaceans, the organization and morphology of the glands that produce it vary considerably among lineages (Sutherland *et al.*, 2010; Walker *et al*., 2015). Nevertheless, similar mechanisms for transforming aqueous protein secretions into solid silk threads have evolved repeatedly, suggesting that silk production may impose common structural constraints on spinning systems. Corophiidans produce a canonical silk that shares key structural and biochemical characteristics with the silks of spiders and moths: semi-cylindrical threads composed of long repetitive proteins which produce semi-crystalline

domains (Kronenberger *et al*., 2012b; McKim & Turner, 2024). But it remains unclear where corophiidan silk-spinning systems fit within the broader diversity of arthropod silk glands. In corophiidans, aqueous silk originates from two types of silk glands, the proximal and distal glands, within the third and fourth pereopods (Fig. 2a). Neretin *et al*. (2017) classified both as pseudotubular glands (Fig. 3b), noting that while they share some features with rosette glands, they are markedly more elongated; Kronenberger *et al.* (2012a) had previously classified the globular proximal glands as lobed (Fig. 3c) and the flower-like distal glands as rosettes (Fig. 3a).

Beyond the glands that produce silk, the morphological structures responsible for transforming and extruding silk remain comparatively poorly understood. Canonical silk production requires specialized extrusion morphology to transform aqueous protein secretions into solid threads. In corophiidans, the reservoir chamber at the dactylus tip is thought to play a central role in conditioning the silk prior to extrusion (Kronenberger *et at*., 2012a; Neretin, 2016). From the glands, aqueous silk travels distally through a series of ductules to the reservoir chamber and then exits a pore on the dactylus surface (Fig. 2a, b) (Kronenberger *et al*., 2012a). Despite its likely importance, the extrusion morphology of corophiidans has received little detailed attention, and the full complement of structures involved in silk transformation remains incompletely described.

To date, silk-spinning systems have been examined in only a handful of corophiidan species and families, making it difficult to determine what the ancestral system looked like or how it has diversified across extant lineages. It has been hypothesized that silk-spinning is ancestral in corophiidans and was lost once in the shared common ancestor of skeleton shrimp (Caprellidae), sea fleas (Podoceridae), and whale lice (Cyamidae) (Myers & Lowry, 2003). This hypothesis is based on the absence of any known silk constructions in these groups. However, the pereopod morphology of these lineages has not been examined, and their phylogenetic relationships remain unresolved. Whether silk-spinning glands and extrusion morphology have truly been lost, and whether any such loss occurred in a single common ancestor, therefore remains an open question.

Here, we conduct an extensive morphological investigation into corophiidan silk-spinning systems and apply phylogenetic comparative methods to their diversification and test whether specific morphological traits and silk types evolve in a correlated manner. We ask the following questions: Do all corophiidans share the same basic morphological elements described in previous literature? Does morphological diversity reflect phylogenetic history? Do specific morphological traits correlate with domicile building behavior? Have silk-spinning glands truly been lost in non-domicile-building lineages?

Materials and methods

Sampling and specimen acquisition

For morphological analysis, we examined 361 pereopods from 40 species representing 13 families and 5 superfamilies within Corophiida (Supplementary Table S1). At least two individuals of each species were examined. When present, pereopods 3 and 4 were dissected and examined for silk-spinning systems and compared with non-silk-producing pereopods (pereopods 2, 5, 6, or 7) from the same individual. Some specimens were collected by authors, and others were acquired on loan from the Natural History Museum of Los Angeles, Santa Barbara Museum of Natural History, Florida Museum of Natural History, and Alabama Museum of Natural History. The collector information and voucher numbers of specimens are available in Supplementary Table S1. Specimens in SM collection were collected with California Department of Fish and Wildlife Scientific Collecting Permit (S-220460007-25002-001).

Microscopy and morphological characterization

To investigate pereopodal glandular systems, we examined pereopods using a combination of light microscopy, confocal scanning laser microscopy, and scanning electron microscopy (SEM). Pereopods were dissected at the top of the basis article, leaving the coxae intact on the body. For light microscopy, whole-mount slides were imaged on an Olympus BX 51 at 4-100x magnification using Lumenera Infinity 3 camera. To resolve topographically complex structures such as the dactylus tip, images were taken at 10-40 µm intervals and compiled into z-project stacks using the brightest point projection method in FIJI (Schindelin *et al*., 2012).

We applied staining protocols for Coomassie brilliant blue (a general protein stain) and bromophenol blue (which targets sulfhydryl, phenolic, and carboxyl groups of proteins) adapted from Kronenberger *et al.* (2012a) and

Bohang (1955), following McKim & Turner (in review) protocol. To establish a staining baseline, we replicated portions of Kronenberger *et al.* (2012a) using taxonomically comparable species: *Americorophium stimpsoni* Shoemaker 1941 and *Monocorophium acherusicum* A. Costa, 1953 (in place of *Crassicorophium bonelli* H. Milne Edwards, 1830) and *Bemlos audbettius* J.L. Barnard, 1962 and *Aoroides secunda* Gurjanova, 1938 (in place of *Lembos websteri* Spence Bate, 1857). We additionally examined species closely related to those in Neretin (2016) and Neretin *et al*. (2017): *Sunamphitoe humeralis* Stimpson, 1864 and *Ampithoe valida* S.I. Smith, 1873 (comparable to *Ampithoe rubricata* Montagu, 1808) and *Dyopedos monocanthus* Metzger, 1875 and *Dulichia sp*. (comparable to *Dyopedos bispinis* Gurjanova, 1930).

For fluorescence microscopy, fresh dissected legs were fixed in 0.4% paraformaldehyde in 1x PBS for one hour, rinsed three times in 1x PBS and preincubated with PBS-TX for 1 hour. Then legs were stained with Hoechst (DAPI; to label nuclei) and phalloidin (to label actin-rich tissue) diluted in 1x PBS for 1 hour, rinsed three times in 1x PBS and rinsed once in 70% glycerol and whole-mounted in 100% glycerol. Slides were imaged on a Leica SP8 confocal microscope at the UCSB NRI-MCDB Microscopy Facility using sequential lasers (DAPI: 350 nm excitation, 461 nm emission, phalloidin: 540 nm excitation, 570 nm emission). When fluorescent staining was not possible, autofluorescence was captured at 488 nm excitation. Z-stacks spanning the dorsal to ventral axis were collected, using Leica Application Suite LAS X, and processed into 3D projections in FIJI.

External morphology was examined by SEM using an FEI Quanta 400F Field emission SEM at the UCSB Department of Earth Science. Specimens were first dehydrated through a stepwise ethanol series, mounted on aluminum stubs with adhesive carbon substrate, and sputtercoated with gold/palladium prior to imaging at 5kV acceleration voltage. Images were collected by a secondary electron signal using an Everhart-Thornley electron detector.

In pereopods 3 and 4, we identified two composite traits of interest: the silk glands in the proximal pereopods that produce aqueous silk products and the silk-extrusion morphology in the dactylus that transforms silk into final extruded products. For the two gland types, proximal and distal, we classified these gland types based on criteria from previous literature (Noirot, 1974; Talbot & Demers, 1993; Kronenberger *et al.*, 2012a; Neretin *et al*., 2017). Glands were classified either as rosette, lobed, or pseudotubular glands (Fig. 3). Lobed glands have one secretory cell with a central duct connecting to the cuticle pore; the secretory cell lining has deep invaginations (Fig. 3a). Rosette glands contain many secretory cells in a rosette (flower-like) organization surrounding an accumulation site that drains into a central duct that connects to the cuticle pore (Fig. 3a). Pseudotubular glands are elongated glands with many secretory cells, which connect to a central duct via a spherical accumulation site and a lateral duct (Fig. 3b).

We also documented the structural diversity of the dactylar silk-extrusion morphology. Previous work has attributed the reservoir chambers as the site where silk is prepared and stored. We therefore gave special attention to the silk-extrusion morphology in the dactylus. In addition, we documented the arrangement of pore types on the dactylus, including slit location, and their spatial relationship to the sensillum groove (a groove with a sensillum sensory setae likely involved in triggering silk). We coded the states of these four silk-spinning morphological characters across lineages: proximal gland presence (0 = absent, 1 = present), distal gland lateral duct morphology (0=absent, 1=simple duct, 2=expanded duct), dactylar slit location (0=slit absent, 1=slit same side of sensillum groove, 2=slit opposite side of sensillum groove), and primary reservoir chamber type (0=absent, 1=typical, 2=modified). Character states scores (Supplementary Table S2) were then used in subsequent phylogenetic analyses.

Character evolution analyses

The genomic corophiidan phylogeny inferred by Cummings (2026) was used for marginal ancestral state reconstruction (ASR). Non-amphipod branches, some non-corophiidan amphipod branches, and branches with multiple individuals of the same species were pruned using ITOL (Letunic & Bork, 2024) prior to ASR to ensure directly comparable traits (Supplementary Figure S3). The pruned tree was converted to an ultrametric chronogram using the *chronos* function in the 'ape' R package (Paradis & Schliep, 2019). We used the *rayDISC* function within the corHMM R package (Beaulieu *et al*., 2013) to test for the best fitting evolutionary model for each character, testing an equal rates (ER) model, an all rates differ (ARD) model, and a symmetrical model (SYM) with a "yang" or a "maddfitz" root prior (Yang, 2006; FitzJohn *et al*., 2009). The best-fitting model was selected based on the lowest

corrected Akaike information criterion (AICc) score. For three of the four characters, distal gland lateral duct morphology, dactylar slit location, and reservoir chamber type, the ER model with a maddfitz root prior provided the best fit. Proximal gland presence was best fit by an ARD model with the same root prior. Character ASR plots were visualized using phytools (Fig. 4) with each node state marginal posterior probability displayed as a piegraph.

Because corophiidan families may produce either homogenous silk or more complex silk with attachment threads, we investigated the relationship between silk extrusion morphology and attachment silk using a cophylogenetic trait analysis and stochastic character mapping in the 'phytools' R package (Revel, 2024). First, we used Pagel's discrete model of correlated trait evolution (Pagel, 1994) to test the independence or dependence of the ecological traits (1) attachment silk; (0) no attachment silk and morphological trait (1) modified chamber; (0) typical chamber. We used an ARD model to capture asymmetry and used the phytools *fitDiscrete* function, which fits Pagel's 1994 model for correlated evolution of two binary, discrete traits. The best model was identified based on the lowest AIC score. We then used stochastic character mapping with 100 simulations and an ARD model to estimate the posterior probabilities of joint trait states (typical chamber with no attachment silk and modified chamber with attachment silk) at internal nodes and along branches.

Results

Dactylar silk-extrusion morphology

We confirmed previously described silk-extrusion structures in pereopods 3 and 4 (Fig. 2b) but also identified undescribed morphological traits and diversity which may influence silk-spinning and secretory products (Fig. 2c). Silk-extrusion traits in the dactylus that remained consistent with previous literature include ductules, a reservoir chamber, a terminal exit pore, and a sensillum groove (Fig. 2b). New traits we have identified include a secondary duct which bypasses the reservoir chamber which has its own chamber, and a slit (Fig. 2c). Old and new structures were found in all examined lineages (excluding the Caprellidae and the Cyamidae) which points to a second distinct secretion system. Additionally, we found distinct variation in the primary reservoir chambers.

Among our most important findings is a set of morphological characters that point to a second silk secretion system. This system is widespread, including in species which have previously been examined, where it seems to have been overlooked. It begins with a secondary duct that originates at the proximal end of the dactylus and runs distally to the tip. It bypasses the ductules and the reservoir chamber and terminates at the dactylar slit (Fig. 5a, c, e). A small secondary chamber is associated with this duct, located distal to the primary chamber. The secondary chamber may be an architectural consequence of the spatial relationship between the primary chamber and the dactylus epidermis rather than a functionally distinct compartment. The secondary duct does not appear to connect with the primary reservoir chamber and instead connects directly to the dactylar slit (Fig. 5 e, f). The position of the slit is distal of the sensillum groove in most species (Fig. 5 a, d), but in the Ischyroceridae (excluding *Notopoma*) and the Podoceridae the slit is positioned on the opposite side of the sensillum groove, adjacent to the exit pore (Fig. 5j, k, l).

We identified substantial structural variation within the primary silk-spinning system as well, which consists of the ductules, reservoir chamber, primary duct, and pore (Fig. 2c). Ductules lead into the reservoir chamber, which then leads to a primary duct that terminates at the exit pore. In the Corophiidae, the Aoridae, the Ischyroceridae, and *Gammaropsis* the reservoir chamber has a simple spindle-shaped morphology (Fig. 5b, c, k) but it was structurally modified in the Ampithoidae, the Dulichiidae, *Notopoma*, and *Photis* (Fig. 5e-i). In the Ampithoidae, the reservoir chamber was composed of a large external chamber and a smaller internal compartment. A subset of ductules entering the reservoir chamber are diverted through three to four small openings into the internal compartment (Fig. 5e). The remaining ductules travel the length of the primary chamber to the exit pore. Products transformed within the internal compartment travel separately down the dactylus before converging with the primary duct proximal to the exit pore.

In *Notopoma*, the modified chamber with an internal compartment resembled the Ampithoidae condition but differed in two respects (Fig. 5g). First, the two ductule bundles were spatially segregated proximal to the chamber. The ductules supplying the internal compartment are physically separate from those delivering products directly to the primary chamber. Second, the entire reservoir chamber narrows sharply before expanding again distally, creating an hourglass constriction. The Dulichiidae exhibited a similarly modified primary chamber, including an internal compartment and distal constriction (Fig. 5h).

The reservoir chamber also contained an internal compartment in *Photis*, but the outer chamber wall formed a rib-like structure encasing both the ductules and the distal primary duct (Fig. 5i). Despite their taxonomic affinity, *Gammaropsis* and *Amphideutopus* lacked this modification, possessing a simple primary chamber more similar to the Aoridae and the Corophiidae – a pattern consistent with their phylogenetic placement (Supplementary Figure S3).

Silk-extrusion morphology was unexpectedly present in the Podoceridae. *Neoxenodice sp.* closely resembled the Ischyroceridae (Fig. 5k) with a simple primary chamber and a dactylar slit positioned opposite the sensillum groove. *Podocerus* was also similar, but the reservoir chamber is positioned extremely close to the exit pore, with no discernible primary duct emerging from the chamber (Fig. 5i).

Silk glands

The morphology of corophiidan silk-spinning glands that we found here is in broad alignment with prior literature. We found two main gland types: a proximal type concentrated in the basis and ischium, and a distal type distributed more abundantly in the ischium, merus, and/or carpus (Fig. 2a). Both proximal and distal glands appeared to be pseudotubular glands. Despite these broad similarities with previous literature, we identified variation in the distal glands across species and a putative third gland type in the Ampithoidae.

In the Corophiidae and the Aoridae, the proximal glands were most densely packed in the basis, ischium, and merus. These glands had irregularly shaped, rounded margins arranged in an acinar configuration and were enclosed by a parental tissue, with characteristically large nuclei and substantial cytoplasm (Fig. 6a, g). We identified channels draining from the secretory cells into a discrete spherical accumulation site, also called spherical structures. The invaginations of the secretory cell lining were weakly developed and the secretory cells connected sequentially to a main duct via lateral ducts. These characters were consistent with pseudotubular glands (Fig. 3b). The proximal glands appeared to connect to the silk-extrusion ductules, reservoir chamber, and terminal pore. While the distal gland appeared to connect to the secondary duct and slit; ducts of both glands traveled from respective glands through subsequent pereopod articles to the dactylus tip (Fig. 2a).

Distal glands in the Corophiidae and the Aoridae were distributed throughout the basis, ischium, merus, and occasionally in the carpus. They shared several features with the proximal glands but were distinguishable by a thin secretory cell lining that stained weakly and had poorly defined boundaries (Fig. 6b, c) and one main central duct connecting all secretory cells. The accumulation sites are conspicuous spheral structures that stain prominently with bromophenol blue and phalloidin (Fig. 6c, f; Supplemental Figure S5 a-e), and the secretory cell lining was typically square-shaped. The tightly clustered draining ductules surround a lateral duct, which produces a superficially rosette-like appearance, but the ultrastructure does not conform to a rosette gland. We observed no cell lining within the draining ductules, no nuclei within the accumulation sites, and one nucleus per cuboid secretory cell (Supplementary Figure S5. a-d). Each distal gland secretory cell's lateral duct connected sequentially to a shared central duct running the length of the leg to the dactylus. Distal gland secretory cells, and corresponding accumulation sites, occurred in two size classes: small and large. Small secretory cells were densely distributed along the midline of the basis (>100 in the basis; Supplementary Figure S5c), while large secretory cells were sparse in the basis (4) and more abundant in the merus (40-60; Supplementary Figure S5a, b), extending into the carpus in the Aoridae (Supplementary Figure S5e).

Glands in the Ampithoidae included proximal and distal glands, but also a third gland type was among the distal glands (Fig. 6i, j). Proximal glands are acinar, lining the perimeter of the basis, with robust secretory cell lining, prominent nuclei, and modest spherical structures (Fig. 6g). The secretory cell lining stains intensely with bromophenol blue, consistent with typical proximal gland morphology. The distal gland occupies the center of the basis and extends into the ischium, merus, and carpus, with weakly staining secretory cell lining (Fig. 6h). The putative third gland type, located within the distal gland region of the basis, is markedly three-dimensional and segmented in appearance (Fig. 6j, k). It resembles the distal glands proximal to them but are compacted into a dense oval cluster of 20-40 secretory cells with each cluster possessing its own central duct.

In the Ischyroceridae (excluding *Notopoma*), gland distribution and types were broadly similar to the Corophiidae and the Aoridae, except the distal gland has expanded lateral ducts (Figs. 3b; 6e, f). Wide lateral ducts

create largely empty gaps beneath the secretory cells which create tissue space through which lateral ducts of adjacent secretory cells are visible.

The Podoceridae also possessed expanded pseudotubular glands with expanded lateral ducts, which are concentrated in the propodus and carpus (Fig. 6k, l). Smaller distal secretory cells are concentrated in the basis, ischium, and merus. Proximal glands appeared to be absent in the Podoceridae.

In the remaining corophiidan lineages, the same proximal and distal gland types and placement were observed (Fig. 9). *Gammaropsis* closely resembled the Aoridae gland configuration while *Photis* possessed additional small distal gland secretory cells in the propodus. In *Notopoma,* proximal glands were largely restricted to the basis, with occasional presence in the carpus. In the Dulichiidae, the narrow pereopods confine proximal glands to the basis, with distal glands present in the merus and carpus. No glandular systems were detected in pereopods 3 and 4 of the Caprellidae species that retain these appendages nor in the remaining pereopods of the Cyamidae (Supplementary Figure S5f).

Additional pereopodal glands

In most species examined, no glands, ducts, or pores were seen in pereopods 2, 5, 6, and 7. In the Ischyroceridae, the Podoceridae, and the Caprellidae, however, glandular systems were found in some of these pereopods. In the pereopod 5 of *Neoxenodice*, small pseudotubular gland secretory cells with simple ducts were present in the basis (Fig. 7a), and large pseudotubular gland secretory cells with expanded lateral ducts were present in the merus and propodus (Fig. 7b); the dactylus of this pereopod also possessed a duct and slit (Fig. 7c). Pereopod 2 of *Neoxendodice* bore large pseudotubular gland secretory cells with simple ducts on the ventral propodus palm (Fig. 7d). In male *Podocerus* large pseudotubular gland secretory cells with expanded lateral ducts were present in pereopod 2.

In male Ischyroceridae (*Jassa marmorata* Holmes, 1905 and *Ericthonius rubricornis* Stimpson, 1983) pereopod 2 contained pseudotubular gland secretory cells with simple lateral ducts within the propodus thumb, appearing connected to secretory pores at the thumb tip (Fig. 7e, f). In male *Caprella* and *Metacaprella*, large rosette glands and large pseudotubular gland secretory cells are present in the ventral palm and dactylus of pereopod 2 (Fig. 7g, h); females possess pseudotubular glands in the ventral palm and rosette glands in the dactylus (Fig. 7i). The caprellid rosette glands are morphologically distinct from pseudotubular glands. Each drain into a single central duct without a spherical accumulation site and has no discernible lateral ducts (Fig. 3a). SEM imaging of pereopod 2 palms revealed numerous fine threads exiting cuticular pores (Fig. 8e, f), but it was unclear if these were directly connected to the pseudotubular glands.

Silk-spinning trait evolution

Ancestral state reconstruction (ASR) supported a single origin of the corophiidan silk-spinning system, with some component traits potentially predating the corophiidan most recent common ancestor (MRCA). The earliest-diverging corophiidan lineages, the Corophiidae and the Aoridae, possess silk-spinning systems most similar to the reconstructed ancestral condition, including proximal glands (posterior probability (pp) = 1.0), distal glands with simple lateral ducts (pp = 0.98), a dactylar slit positioned on the same side as the sensillum groove (pp = 0.98), and a simple reservoir chamber (pp = 0.93) (Fig. 4. a-d; Fig. 9).

Within corophiidans, proximal glands were subsequently lost in *Podocerus* MRCA (pp = 0.75) and independently in *Neoxenodice*. All silk-spinning traits were lost in the Caprellidae, coincident with the reduction or complete loss of pereopods 3 and 4. Distal glands with expanded lateral ducts originated once in the MRCA of Podoceridae and Ischyroceridae (pp = 0.98), as did the transposition of the dactylar slit to the side opposite the sensillum groove (pp = 0.99). The origin of the modified chamber remains poorly resolved: the posterior probability of this trait being present in the MRCA of the Ampithoidae and *Photis* (pp = 0.54) and the MRCA of *Notopoma* and Dulichiidae (pp = 0.58) were low.

Modified reservoir chambers were strongly associated with the production of attachment silk, evolving in a correlative manner. Pagel's test for correlated evolution indicated that the evolution of these two traits were highly dependent (Pagel's test: dependent model AIC= 34.5, independent model AIC = 47.1), with transitions occurring in a strictly correlated and irreversible manner: modified chambers and attached silk always co-originated, with no

reversals detected (p-value: 0.00037). Across 100 stochastic character mapping simulations, an average of 3.13 transitions from absence of both traits (0|0) to the presence of both (1|1) were recovered, though the placement of these transitions was inconsistent across simulations and reconstructed with low node-level confidence. Posterior probability of a 1|1 state was low at both the MRCA of *Notopoma* and Dulichiidae (pp = 0.40) and the MRCA of *Photis* and Ampithoidae (pp = 0.45), but increased substantially toward the tips (Supplementary Figure S6).

Discussion

Corophiidans exhibit remarkable diversity in both morphology and lifestyle, making them an ideal system for examining the evolution of arthropod silk production. Our results support silk-spinning as an ancestral trait within Corophiida and reveal extensive diversification of silk-spinning morphology across extant lineages (Fig. 9). Most corophiidans retain a conserved silk-spinning architecture in pereopods 3 and 4 consisting of pseudotubular glands and specialized dactylar silk-extrusion structures. However, species vary in the lateral duct type in distal glands, dactylus slit location, reservoir chamber type, and retention of proximal glands. Building on previous studies, we reclassify corophiidan gland types and identify several previously undescribed silk-extrusion characters, including the secondary duct, secondary chamber, dactylar slit, and internal compartment associated with modified reservoir chambers. Together, these findings demonstrate that corophiidan silk-spinning systems are more morphologically complex and evolutionarily labile than previously recognized.

Several newly recognized silk-extrusion structures provide new insights into how corophiidans process and secrete silk. Previous studies of the Aoridae, the Corophiidae, and the Ampithoidae have alluded to a secondary duct and slit, but these structures have not been formally characterized. In Kronenberger *et al*. (2012a) a TEM micrograph of *Crassicorophium bonellii* shows an "unidentified structure" running distal to the sensillum groove with apparent secreted material. We interpret this structure as the secondary duct and dactylar slit found in our study. This interpretation is further supported by SEM images in Kronenberger *et a*l. (2012a) which show secreted material on the dactylar tip opposite side of the pore, consistent with external secretion from the slit. The dactylar slit is an elongated opening that likely influences the structure or diameter of the thread differentially to a circular pore. Some species of spiders use an elongated, flattened slit which alternatively creates ribbon-like threads rather than semi-cylindrical threads (Knight & Vollrath, 2002). In silk moths, duct and pore geometry influences thread production (Huang *et al*., 2025) and in some spiders, silk spigot diameter and pressure can be intentionally altered to affect silk thread properties (Wilson, 1969).

The presence of two distinct pathways of silk secretion – the exit pore and the newly described dactylar slit – suggests that some products do not mix prior to extrusion. This contrasts with previous work (Kronenberger *et al.*, 2012a; Neretin, 2016) which found that both proximal and distal glands mix in the reservoir chamber. Recognizing these two unique glandular systems in pereopods 3 and 4 is important for understanding the evolutionary origin of these glands. A parallel can be drawn with spiders, where each gland type has its own unique exit pore (or spigot), and orb-weaving spiders can possess up to seven gland types that are derived from the duplication of an ancestral silk gland (Marples, 2008). In spiders, the silk gene family and its resulting silk proteins have co-evolved with gland specialization (Hayashi & Lewis, 1998). A similar scenario may have occurred in amphipod silk glands, with one gland type duplicating from an ancestral version and subsequently diversifying and specializing. Whether the proximal or distal glands represent the ancestral condition in corophiidans remains an open question. When examining the Ampeliscidae and closely related outgroups, glands which resemble the distal glands in corophiidans were found in all species, suggesting that those glands may be the ancestral type (McKim & Turner, in review).

Repeated modifications of the primary reservoir chamber appear to have played a central role in the evolution of attachment silk. In lineages with modified primary chambers, including the Ampithoidae, *Photis, Notopoma*, and the Dulichiidae, species can produce an attachment silk used to anchor domiciles to the substrate, a behavior not yet demonstrated in other lineages. This attachment silk appears whiter and stronger than other threads produced by the same individual (Fig. 1). The modified chambers may facilitate the transformation of silk from a liquid to a solid in a way that produces these distinct mechanical properties. The modified chambers of *Notopoma* and the Dulichiidae, which contain an hourglass constriction, are reminiscent of the anterior segment of the silk glands in silk moth caterpillars. In the silk gland anterior segment, a thickened cuticle lining creates an hourglass constriction that tapers

until the exit pore. This structure, termed the cuticular intima, plays a critical role in producing viable silk threads by forcing the transformation of liquid silk proteins into solid semi-crystalline threads (Wang *et al.*, 2022; Huang *et al*., 2025). The hourglass constriction in *Notopoma* and Dulichiidae may play a similar role in silk transformation.

Our trait analyses support a scenario in which the correlated evolution of modified reservoir chambers and attachment silk production occurred convergently four times across corophoid lineages. The repeated origin of this trait combination suggests that producing attachment silk imposes a shared functional demand that the reservoir chamber is uniquely positioned to meet. Remarkably, each lineage appears to have arrived at a structural solution: the internal chamber of the Ampithoidae diverts and separately processes a subset of ductule products; *Notopoma* achieves additional transformation through a pronounced hourglass constriction; Dulichiidae combines an internal compartment with a similar constriction; and *Photis* encases its ductules and internal chamber in a rib-like outer wall. Because of this convergence, one can speculate that the chamber is a critical locus for producing the mechanical properties that define attachment silk. This pattern parallels convergent evolution in spider silk gland systems, where independent lineages have modified gland architecture and produce functionally analogous silk types (Wolff *et al*., 2024). This raises the question of whether conserved developmental or biochemical mechanisms underlie the observed convergent structural modifications.

These chamber modifications may also provide phylogenetically informative characters. For example, it was initially unexpected that *Notopoma* fell outside the Ischyroceridae clade (Supplementary Figure S3). However, the silk-spinning morphology of this genus more closely resembles that of the Dulichiidae than the Ischyroceridae, lending independent morphological support for this phylogenetic arrangement.

In addition to modified chambers, the Ampithoidae possesses unique glands that may represent a third gland type, with implications for the diversity of silk produced. Cerda *et al.* (2010) found that Ampithoidae produces multiple types of silk in its kelp domiciles, and a third gland type could account for the unusually high abundance of strong attachment threads in this group compared to other corophiidan lineages.

In addition to reservoir chamber evolution, the secondary secretion system also diversified across corophiidan lineages. In the Ischyroceridae (excluding *Notopoma*) and the Podoceridae, the slit location has shifted to the opposite side of the sensillum groove, where it is adjacent to the pore (Fig. 5j-l). The dactylar slit is associated with the distal glands so it may be that this positional shift is correlated to the origin of distal glands with expanded lateral ducts, occurring in the MRCA of Ischyroceridae and Podoceridae (Fig. 9). How this rearrangement affects secretion performance and function remains to be investigated.

The retention of silk-spinning morphology in the Podoceridae suggests that the loss of domicile-building behavior does not necessarily entail the loss of silk production. Previous phylogenetic analyses inferred that domicile-building behavior was lost in *Podocerus* and *Neoxenodice* despite the ancestral presence of silk-spinning within Corophiida (Cummings, 2026). However, both genera retain silk-spinning structures, indicating that the underlying secretory apparatus persists despite the apparent loss of silk constructions. The divergent function of the silk-spinning system may instead serve as camouflage or defense. This hypothesis is supported by the observation of amorphous and thread-like secretions coating the body of *Podocerus* (Fig. 8a-c), which appeared to facilitate the adhesion of detritus to the cuticle. Specimens of the Podoceridae were covered in more detritus than any other corophiidan lineage examined. The loss of proximal glands in *Podocerus* and *Neoxenodice* likely constrains the products available to these animals and may underlie their distinct natural histories. In spiders, gland loss has been associated with shifts in silk use and natural history (Griswold *et al*., 1998; Berger *et al.*, 2021), and a similar relationship may exist here.

While silk-spinning morphology is absent from pereopods 3 and 4 in the Caprellidae, the presence of glandular systems in pereopod 2 suggest that secretory capacity has been redirected rather than simply lost. In male *Caprella* and *Metacaprella*, large rosette glands secrete from a palmar “poison tooth” (Lim & Alexander, 1986; Schulz & Alexander, 2001; Matthews, 2008) through groups of pores on both sides of the tooth (Takeshita & Wada, 2012). This poison tooth appears to function in male-male competition and has been implicated in causing death through potential toxic mechanisms (Matthews, 2008). Further research is needed to test the identity of the poison tooth rosette glands secretions. The prevalence and function of rosette glands across the Caprellidae are incompletely understood and deserve further investigation.

Comparisons with independently evolved silk-spinning systems provide additional insight into the evolutionary origin of corophiidan silk-spinning morphology. Primary chambers were initially thought to be unique to corophiidan amphipods. However, they have recently been identified in silk-spinning systems of the Ampeliscidae amphipods (McKim & Turner, in review), suggesting that the capacity to transform and manipulate silk within a chamber may be more widespread than previously recognized. Likewise, glands resembling corophiidan distal glands occur throughout pereopods of the Ampeliscidae and closely related outgroups, suggesting that distal glands may represent the ancestral gland type. Together, these observations indicate that key components of the corophiidan silk-spinning system may have deeper evolutionary origins within Amphipoda than previously appreciated.

The evolutionary relationship between rosette and pseudotubular glands remains unresolved. In contrast to the Caprellidae, rosette glands were not found in pereopod 2 of the closely related groups, the Ischyroceridae and the Podoceridae. Instead, large pseudotubular gland secretory cells are present in the same location in the ventral propodus of males (Fig. 8e, f). This pattern raises the possibility that the potentially venomous rosette glands in the Caprellidae evolved from ancestral pseudotubular glands. Alternatively, both proximal and distal pseudotubular glands may have evolved from ancestral rosette glands that elongated and developed additional ultrastructures over time, as proposed by Neretin *et al*., 2017. Similar pseudotubular-like glands have been found in pereopod 2 of the Dulichiidae (Mattson & Cedhagen, 1989), but the distribution of this condition across Corophiida remains poorly understood. The discovery of pseudotubular glands throughout all pereopods of the Ampeliscidae, which sometimes produce threads from cuticular pores (McKim & Turner, in review), further suggests that pseudotubular glands may represent an ancient amphipod feature that preceded and facilitated the evolution of dedicated silk-spinning systems. If so, the evolutionary origins of amphipod silk production may extend substantially deeper than previously recognized, with dedicated silk-spinning systems arising through the modification and specialization of pre-existing secretory structures.

Conclusion

This study represents the most extensive morphological survey of Corophiida silk-spinning systems to date, and its findings substantially enhance our understanding of how amphipods produce, modify and deploy silk. We document a shared, conserved silk-spinning system that has evolved and diversified into structural elaborations specific to certain lineages. The newly described structures reported here reframe how silk extrusion has been interpreted in previous work and implicate unrecognized systems in the transformation of silk products prior to extrusion. Most strikingly, modified reservoir chambers and the production of strong attachment silk co-evolved in a strictly correlated and irreversible manner, arising independently at least four times, each time through a distinct structural modification of the same glandular component. Even lineages historically assumed to have lost silk entirely, such as the Podoceridae, retain silk-spinning morphology. This underscores that the absence of tube-building behavior cannot be taken as evidence for the absence of silk, opening the door for future natural history studies. These findings establish corophiidan amphipods as a compelling comparative system for studying the evolution of biological adhesives and structural silk, with parallels to spider silk diversification. The morphological diversity uncovered here opens as many questions as it answers, particularly regarding the functional significance of dual-secretion pathways and the identity of the ancestral amphipod silk gland. This sets the foundation for the next generation of investigations into amphipod silk biology and evolution of silk in arthropods.

Data Availability

Original and pruned phylogeny available on github, as well as character state tables, and an R script with the ancestral state reconstruction and correlative trait modeling: github.com/coding4amphipods/Corophiida

References

Alderman, A.L. 1936. Some new and little known ampipods of California. University of California Publications in Zoology, 41, 53-74.

Barnard, J.L. 1954. A new species of Microjassa from Los Angeles Harbor. *Bulletin of the Southern California Academy of Sciences,* 53, 127-130

Barnard, J.L. 1962. Benthic marine Amphipoda of southern California 1. Families Aoridae, Photidae, Ischyroceridae, Corophiidae, Podoceridae. *Pacific Naturalist,* 3(1), 1-72.

Barnard, J. L. 1969. A biological survey of Bahia de Los Angeles Gulf of California, Mexico, IV. Benthic Amphipoda (Crustacea). *Transactions of the San Diego Society of Natural History.* 15, 175-228. https://doi.org/10.5962/bhl.part.12057

Barnard, J. L.; Reish, D. J. 1959. Ecology of Amphipoda and Polychaeta of Newport Bay, California. *Allan Hancock Foundation Publications, Occasional Paper,* 1-106.

Bate, C. S. 1857. A synopsis of the British edriophthalmous Crustacea. Part I. Amphipoda. *The Annals and Magazine of Natural History, series 2,* 19, 135-152. https://doi.org/10.1080/00222935708697715

Beaulieu, J.M., O'Meara, B.C. & Donoghue, M.J. 2013. Identifying Hidden Rate Changes in the Evolution of a Binary Morphological Character: The Evolution of Plant Habit in Campanulid Angiosperms. *Systematic Biology*, 62, 725–737. https://doi.org/10.1093/sysbio/syt034

Berger, C.A., Brewer, M.S., Kono, N., Nakamura, H., Arakawa, K., Kennedy, S.R., Wood, H.M., Adams, S.A. & Gillespie, R.G. 2021. Shifts in morphology, gene expression, and selection underlie web loss in Hawaiian Tetragnatha spiders. *BMC Ecology and Evolution*, 21, 48. https://doi.org/10.1186/s12862-021-01779-9

Carter, J.W. 1982. Natural History Observations on the Gastropod Shell-Using Amphipod Photis Conchicola Alderman, 1936. *Journal of Crustacean Biology*, 2, 328–341. https://doi.org/10.2307/1548051

Cerda, O., Hinojosa, I.A. & Thiel, M. 2010. Nest-Building Behavior by the Amphipod *Peramphithoe femorata* (Krøyer) on the Kelp *Macrocystis pyrifera* (Linnaeus) C. Agardh From Northern-Central Chile. *The Biological Bulletin*, 218, 248–258. https://doi.org/10.1086/BBLv218n3p248

Conlan, K.E. 1990. Revision of the crustacean amphipod genus Jassa Leach (Corophioidea: Ischyroceridae). *Canadian Journal of Zoology,* 68, 2031-2075. https://doi.org/10.1139/z90-288

Costa, A. 1853. Relazione sulla memoria del Dottor Achille Costa, di Ricerche su' Crostacei Amfipodi del Regno di Napoli. *Rendiconti della Societa Reale Borbonica, Accademia delle Scienze, new series,* 2, 167-178. https://www.biodiversitylibrary.org/page/7473465

Craig, C.L. 1997. Evolution of arthropod silks. *Annual Review of Entomology*, 42, 231–267. https://doi.org/10.1146/annurev.ento.42.1.231

Cummings. B.M. 2026. Unraveling amphipod diversity across phylogenetic, phenotypic, and community scales (Doctoral dissertation, University of Florida). https://ufdc.ufl.edu/UFE0063438/00001

Dana, J.D. 1853 - 1855. Crustacea. Part II. *In: United States Exploring Expedition. During the years 1838, 1839, 1840, 1841, 1842. Under the command of Charles Wilkes. U. S. N., C. Sherman Printer, Philadelphia.* 14, 691-1618.

Gorvett, H. 1952. The Tegumental glands in the land Isopoda: C. the lobed glands: the Properties of their secretion and their mode of action. *Journal of Cell Science*, S3–93, 17–29.

Griswold, C.E., Coddington, J.A., Hormiga, G. & Scharff, N. 1998. Phylogeny of the orb-web building spiders (Araneae, Orbiculariae: Deinopoidea, Araneoidea). *Zoological Journal of the Linnean Society*, 123, 1–99. https://doi.org/10.1111/j.1096-3642.1998.tb01290.x

Gurjanova, E. 1930. Beiträge zur Fauna der Crustacea-Malacostraca des arktischen Gebietes. *Zoologischer Anzeiger,* 86, 231-248.

Gurjanova, E. 1938. Amphipoda, Gammaroidea zalikov Siaukhu i Sudzukhe (Yaponskoe More). *Reports of the Japan Sea Hydrobiological Expedition of the Zoological Institute of the Academy of Sciences USSR in 1934,* 1, 241-404.

FitzJohn, R.G. Maddison, W.P., & Otto, S.P. 2009. Estimating trait-dependent speciation and extinction rates from incompletely resolved phylogenies. *Systematic Biology*, 58, 595-611. https://doi.org/10.1093/sysbio/syp067

Hayashi, C.Y. & Lewis, R.V. 1998. Evidence from flagelliform silk cDNA for the structural basis of elasticity and modular nature of spider silks. *Journal of Molecular Biology*, 275, 773–784. https://doi.org/10.1006/jmbi.1997.1478

Holmes, S. J. 1905. The Amphipoda of southern New England. Bulletin of the United States. *Bureau of Fisheries,* 24, 457-529. https://www.biodiversitylibrary.org/page/25135693

Huang, Q., Hu, X., Fan, X., Li, Y., Wei, M., Li, X., Liu, K., Lin, Z., Li, Y., Dong, Z., Zhao, P., Xia, Q. & Wang, X. 2025. Longer Duct, Better Silk: Unveiling How Anterior Silk Gland Length Boosts Fiber Performance. *Biomacromolecules*, 26, 4262–4273. https://doi.org/10.1021/acs.biomac.5c00275

Kakui, K., Fleming, J.F., Mori, M., Fujiwara, Y. & Arakawa, K. 2021. Comprehensive Transcriptome Sequencing of Tanaidacea with Proteomic Evidences for Their Silk. *Genome Biology and Evolution*, 13, evab281. https://doi.org/10.1093/gbe/evab281

Kakui, K. & Hiruta, C. 2014. Diverse pereopodal secretory systems implicated in thread production in an apseudomorph tanaidacean crustacean. *Journal of Morphology*, 275, 1041–1052. https://doi.org/10.1002/jmor.20281

Knight, D.P. & Vollrath, F. 2002. Spinning an elastic ribbon of spider silk. *Philosophical Transactions of the Royal Society B: Biological Sciences*, 357, 219–227. https://doi.org/10.1098/rstb.2001.1026

Kronenberger, K., Moore, P.G., Halcrow, K. & Vollrath, F. 2012a. Spinning a marine silk for the purpose of tube-building. *Journal of Crustacean Biology*, 32, 191–202.

Kronenberger, K., Dicko, C., & Vollrath, F. 2012b. A novel marine silk. *Naturwissenschaften*, *99*(1), 3–10. https://doi.org/10.1007/s00114-011-0853-5

Kröyer, H. 1838. Grönlands Amfipoder. *Det Konigelige Danske Videnskabernes Selskabs Naturvidenskabelige og Mathematiske Afhandlinger, series 4,* 7, 229-326.

Laubitz D.R. 1970. Studies on the Caprellidae (Crustacea, Amphipoda) of the American North Pacific. National Museums of Canada, Publications in Biological Oceanography, 1, 1-89.

Letunic, I. & Bork, P. 2024. Interactive Tree of Life (iTOL) v6: recent updates to the phylogenetic tree display and annotation tool. *Nucleic Acids Research*, 52, W78–W82. https://doi.org/10.1093/nar/gkae268

Lim, S.T.A. & Alexander, C.G. 1986. Reproductive behaviour of the caprellid amphipod, Caprella Scaura Typica, Mayer 1890. *Marine Behaviour and Physiology*, 12, 217–230. https://doi.org/10.1080/10236248609378648

Lütken, C. 1870. Conspectus Cyamidarum borealium hujusque cognitarum. Forhandlinger i Videnskabs-Selskabet i. *Christiana,* 279-280. https://archive.org/details/biostor-101947/mode/2up

Marples, B.J. 1967. The spinnerets and epiandrous glands of spiders. *Zoological Journal of the Linnean Society*, 46, 209–222. https://doi.org/10.1111/j.1096-3642.1967.tb00504.x

Matthews, S.L. 2008. Maternal care, male-male aggression, and the use of a specialized appendage in the Caprellid amphipod, Caprella mutica, (Doctoral dissertation, University of Oregon). https://scholarsbank.uoregon.edu/server/api/core/bitstreams/49a8baa6-e9f5-4978-8ee4-7d6a9effa307/content

Mattson, S. & Cedhagen, T. 1989. Aspects of the behaviour and ecology of Dyopedos monacanthus (Metzger) and D.porrectus Bate, with comparative notes on Dulichi tuberculata Boeck (Crustacea : Amphipoda : Podoceridae). Journal of Experimental Marine Biology and Ecology, 127, 253-272.

Mayer P. 1890. Die Caprelliden des Golfes von Neapel und der angrenzenden meeres-abschnitte. Nachtrag zur monographie derselben. *Fauna und Flora des Golfes von Neapel und der angrenzenden Meeres-Abschnitte*, 17, 1-157. https://www.biodiversitylibrary.org/bibliography/53624#/summary

Mayer, P. 1903. Die Caprellidae der Siboga-Expedition. *Siboga-Expeditie. Uitkomsten op zoologisch, botanisch, oceanographisch en geologisch gebied verzameld in Nederlandsch Oost-Indie 1899-1900 aan boord H.M. Siboga,* 34. https://biodiversitylibrary.org/page/37095363

McCain, John C. 1968 The Caprellidae (Crustacea, Amphipoda) of the Western North Atlantic, *Bulletin of the United States National Museum*, 278, 1-115. https://doi.org/10.5962/bhl.part.8960

McKim, S.A. & Turner, T.L. 2024. The evolution of silk production in Crustacea. *Journal of Crustacean Biology*, 44, ruae056. https://doi.org/10.1093/jcbiol/ruae056

McKim, S.A. & Turner, T.L. *in review*. Comparative morphology of silk-spinning systems in amphipods. bioRxiv [preprint] doi: https://doi.org/10.64898/2026.05.07.723571

Metzger A. 1875. Crustaceen aus den Ordnungen. Edriophthalmata und Podophthalmata. Zoologische Ergebnisse der Nordseefahrt vom 21 Juli bis 9 September 1872. *Jahresbericht der Commission zur Wissenschaftlichen Untersuchung der Deutschen Meere*, 2-3, 277-309. https://doi.org/10.5962/bhl.title.10251

Milne Edwards, H. 1830. Extrait de recherches pour servir à l'histoire naturelle des crustacés amphipodes. *Annales des Sciences Naturelles,* 20, 353-399. https://www.biodiversitylibrary.org/page/6069923

Montagu, G. 1808. Description of several marine animals found on the south coast of Devonshire. *Transactions of the Linnean Society of London,* 9, 81-114. https://www.biodiversitylibrary.org/page/757838

Neretin, N.Y., Zhadan, A.E. & Tzetlin, A.B. 2017. Aspects of mast building and the fine structure of "amphipod silk" glands in *Dyopedos bispinis* (Amphipoda, Dulichiidae). *Contributions to Zoology*, 86, 145–168. https://doi.org/10.1163/18759866-08602003

Neretin, N.Y. 2016. The morphology and ultrastructure of "amphipod silk" glands in Ampithoe rubricata (Crustacea, Amphipoda, Ampithoidae). *Biology Bulletin*, 43, 628–642. https://doi.org/10.1134/S106235901607013X

Noirot, C. & Quennedey, A. 1974. Fine Structure of Insect Epidermal Glands. *Annual Review of Entomology*, 19, 61–80. lhttps://doi.org/10.1146/annwiurev.en.19.010174.000425

Pagel, M. 1994. Detecting correlated evolution on phylogenies: A general method for the comparative analysis for discrete characters. *Proceedings of the Royal Society B*, 255, 37-45.

Paradis, E. & Schliep, K. 2019. ape 5.0: an environment for modern phylogenetics and evolutionary analyses in R. *Bioinformatics*, 35, 526–528. https://doi.org/10.1093/bioinformatics/bty633

Reboleira, A.S.P.S. & Enghoff, H. 2016. Mud and silk in the dark: A new type of millipede moulting chamber and first observations on the maturation moult in the order Callipodida. *Arthropod Structure & Development*, 45, 301–306. https://doi.org/10.1016/j.asd.2016.04.001

Revell LJ. 2024. phytools 2.0: an updated R ecosystem for phylogenetic comparative methods (and other things) *PeerJ,* 12, e16505. https://doi.org/10.7717/peerj.16505

Robson, S.K.A., Kohout, R.J., Beckenbach, A.T. & Moreau, C.S. 2015. Evolutionary transitions of complex labile traits: Silk weaving and arboreal nesting in Polyrhachis ants. *Behavioral Ecology and Sociobiology*, 69, 449–458. https://doi.org/10.1007/s00265-014-1857-x

Schellenberg, A. 1925. Die Amphipodengattung Ampelisca und das Bipolaritatsproblem Zoologischer Anzeiger. *Zoologischer Anzeiger.* 62, 125-129.

Schellenberg, A. 1926. Die Caprelliden und Neoxenodice caprellinoides n.g. s.sp. der Deutschen Sudpolar-Expedition 1901-1903. *Deutsche Sudpolar-Expedition 1901-1903,* 18, 463-476.

Schellenberg, A. 1926. Die Gammariden der Deutschen Sudpolar-Expedition 1901-1903. *Deutsche Sudpolar-Expedition 1901-1903,* 1,: 235-414.

Schellenberg, A. 1931. Gammariden und Caprelliden des Magellangebietes, Sudgeorgiens und der Westantarktis. *Further Zoological Results of the Swedish Antarctic Expedition, 1901-1903,* 6, 1-290.

Schurin, A. 1935. Zur Fauna der Caprelliden der Bucht Peters der Grosse (Japanisches Meer. *Zoologischer Anzeiger,* 112, 198-203.

Schulz, M.K. & Alexander, C.G. 2001. Aggressive behaviour of *caprella scaura typica* mayer, 1890. (crustacea: Amphipoda). *Marine and Freshwater Behaviour and Physiology*, 34, 181–187. https://doi.org/10.1080/10236240109379071

Shillaker, R.O. & Moore, P.G. 1978. Tube building by the amphipods Lembos websteri Bate and Corophium bonnellii Milne Edwards. *Journal of Experimental Marine Biology and Ecology*, 33, 169–185. https://doi.org/10.1016/0022-0981(78)90006-0

Shillaker, R.O. & Moore, P.G. 1987. Tube-emergence behaviour in the amphipods Lembos websteri Bate and Corophium bonnellii Milne Edwards. *Journal of Experimental Marine Biology and Ecology*, 111, 231–241. https://doi.org/10.1016/0022-0981(87)90030-X

Shoemaker C.R. 1941. A new genus and new species of Amphipoda from the Pacific Coast of North America. *Proceedings of the Biological Society of Washington*, 54, 183-186.

Skutch, A.F. 1926. On the Habits and Ecology of the Tube-Building Amphipod Amphithoe Rubricata Montagu. *Ecology*, 7, 481–502. https://doi.org/10.2307/1931173

Smith, S. I. 1873. Crustacea, ex. Isopoda. In: AE. Verrill's "Report upon the invertebrate animals of Vineyard Sound .... " U.S. Commission of Fish and Fisheries. Pt. 1. Report on the Condition of the Sea Fisheries of the South Coast of New England in 1871 and 1872. 295-778.

Souza-Filho, J.F.; Souza, A.M.T.; Valério-Berardo, M.T. 2010. Six new species of the genus Chevalia Walker, 1904 (Amphipoda, Corophiidea, Chevaliidae) from Brazilian waters, with a key to world species of the genus. *Zootaxa,* 2713, 25-51. https://doi.org/10.11646/zootaxa.2713.1.2

Stephensen K. 1938. Grandidierella japonica n. sp., a new amphipod with stridulating organs from brackish water in Japan. *Annotationes Zoologicae Japonenses*., 17, 179-184

Stimpson, W. 1853. Synopsis of the marine Invertebrata of Grand Manan: or the region about the mouth of the Bay of Fundy, New Brunswick. *Smithsonian Contributions to Knowledge,* 6, 1-66. https://www.biodiversitylibrary.org/page/32536624

Stimpson, W. 1856. On some Californian Crustacea. *Proceedings of the California Academy of Sciences,* 1, 87-90.

Stimpson, W. 1864. Descriptions of new species of marine Invertebrata from Puget Sound, collected by the naturalists of the North-West Boundary Commission, A.H. Campbell, Esq., Commissioner. *Proceedings of the Academy of Natural Sciences of Philadelphia,* 16, 153-161. http://biodiversitylibrary.org/page/1942749

Sutherland, T.D., Young, J.H., Weisman, S., Hayashi, C.Y. & Merritt, D.J. 2010. Insect Silk: One Name, Many Materials. *Annual Review of Entomology*, 55, 171–188. https://doi.org/10.1146/annurev-ento-112408-085401

Takeshita, F. & Wada, S. 2012. Morphological Comparison of the Second Gnathopod in Males of Four Caprellid Species (Amphipoda: Caprellidae). *Journal of Crustacean Biology*, 32, 673–676. https://doi.org/10.1163/193724012X637320

Talbot, P., & Demers, D. (1993). Tegumental glands of Crustacea. The crustacean integument: morphology and biochemistry. *CRC Press, New York*, 151-191.

Thomson, G.M. 1879. Additions to the amphipodous Crustacea of New Zealand. *Annals and Magazine of Natural History,* 5, 329-333. https://doi.org/10.1080/00222937908679843

Tuchina, O., Groh, K.C., Talarico, G., Müller, C.H.G., Wielsch, N., Hupfer, Y., Svatoš, A., Grosse-Wilde, E. & Hansson, B.S. 2014. Morphology and Histochemistry of the Aesthetasc-Associated Epidermal Glands in Terrestrial Hermit Crabs of the Genus Coenobita (Decapoda: Paguroidea). *PLoS ONE*, 9, e96430. https://doi.org/10.1371/journal.pone.0096430

Walker, A.A., Holland, C. & Sutherland, T.D. 2015. More than one way to spin a crystallite: multiple trajectories through liquid crystallinity to solid silk. *Proceedings of the Royal Society B: Biological Sciences*, 282, 20150259. https://doi.org/10.1098/rspb.2015.0259

Walker, A.O. 1898. Crustacea collected by W.A. Herdman, F.R.S., in Puget Sound, Pacific coast of North America, September 1897. *Proceedings of the Liverpool Biological Society,* 12, 268-287.

Wang, X., Xie, X., Xie, K., Liu, Q., Li, Y., Tan, X., Dong, H., Li, X., Dong, Z., Xia, Q. & Zhao, P. 2022. Chitin and cuticle proteins form the cuticular layer in the spinning duct of silkworm. *Acta Biomaterialia*, 145, 260–271. https://doi.org/10.1016/j.actbio.2022.03.043

Wigley, R. L. 1966. Two new marine amphipods from Massachusetts, U.S.A. *Crustaceana,* 10, 259-270. https://www.jstor.org/stable/20102746

Wilson, R.S. 1969. Control of Drag-Line Spinning in Certain Spiders. *American Zoologist*, 9, 103–111. https://doi.org/10.1093/icb/9.1.103

Wolff, J.O., Ashley, L.J., Schmitt, C., Heu, C., Denkova, D., Jani, M., Řezáčová, V., Blamires, S.J., Gorb, S.N., Garb, J., Goodacre, S.L. & Řezáč, M. 2024. From fibres to adhesives: evolution of spider capture threads from web anchors by radical changes in silk gland function. *Journal of The Royal Society Interface*, 21, 20240123. https://doi.org/10.1098/rsif.2024.0123

Yang, Z. 2006. Computational Molecular. Oxford University Press

Acknowledgments

We thank Christoph Pierre and Christian Orsini at UCSB for helping to collect California amphipod specimens, Regina Wetzer for loaning specimens from the Los Angeles Natural History Museum, Vanessa Delnavaz for loaning specimens from the Santa Barbara Museum of Natural History, and Gustav Paulay for loaning specimens from the Florida Museum of Natural History. Thanks to Dexter Davies for sharing specimens from Antarctica and to Inez Mangino for sharing caprellid specimens. Thanks to Elyse Wurster & Kerri Danil at the Southwest Fisheries Science Center National Marine Fisheries Service for obtaining and sharing whale lice specimens. Thanks to Jacob Gorneau for help with correlative evolution analyses and to Lisa Mesrop for help with fluorescent staining protocols. Thanks to Lewis "Lee" Sharpnack and Gareth Seward at the UCSB Earth Science Electron Microscopy and Microanalysis Lab for their assistance with SEM data collection. Thanks to Benjamin Lopez at the NRI-MCDB Microscopy Facility for microscope training and assistance. We acknowledge the use of the NRI-MCDB Microscopy Facility and the Resonant Scanning Confocal supported by the NSF MRI grant DBI-1625770.

Funding and Competing Interests

Financial support was provided by NSF-GRFP (22-614), UCSB Coastal Fund Grants (CF-202501-12007 & CF-202404-09789), the 2024 American Microscopy Society Graduate Student Award, the 2024 Society of Systematic Biologist Graduate Student Award and the American Museum of Natural History 2024 Lerner-Gray Fund for Marine Research.

Author Information

Authors and Affiliations

Ecology, Evolution, and Marine Biology Department, University of California, Santa Barbara, CA 93106, USA
Siena A. McKim, Thomas L. Turner, Siena E. Waldman

Florida Museum of Natural History, University of Florida, Gainesville, FL 32611, USA
Brittany M. Cummings

Minderoo-UWA Deep-Sea Research Centre, The University of Western Australia, WA 6009, Australia
Antonia M. Johnstone

Natural History Museum of Los Angeles County, Los Angeles, CA 90007, USA
Adam R. Wall

Department of Biological Science, University of Alabama, Tuscaloosa, AL 35473 USA
Kevin M. Kocot

Contributions
Conceptualization: S.M.; Methodology: S.M., B.C., S.W., ; Formal analysis and investigation: S.M., B.C.; Writing - original draft preparation: S.M.; Writing - review and editing: S.M., B.C., S.W., A.J., A.W., K.K., T.T.; Visualization: S.M.; Funding acquisition: S.M.; Resources: S.M., B.C., K.K., A.W, T.T.; Supervision: K.K., T.T.

Corresponding author
Correspondence to Siena A. McKim, e-mail: smckim@ucsb.edu

Declarations

Ethics Declarations
No approval of research ethics committees was required to accomplish the goals of this study because experimental work was conducted with unregulated invertebrate species.

Conflicts of interest
The authors declare they have no financial interests and no competing interests to declare that are relevant to the content of this article.

Figure

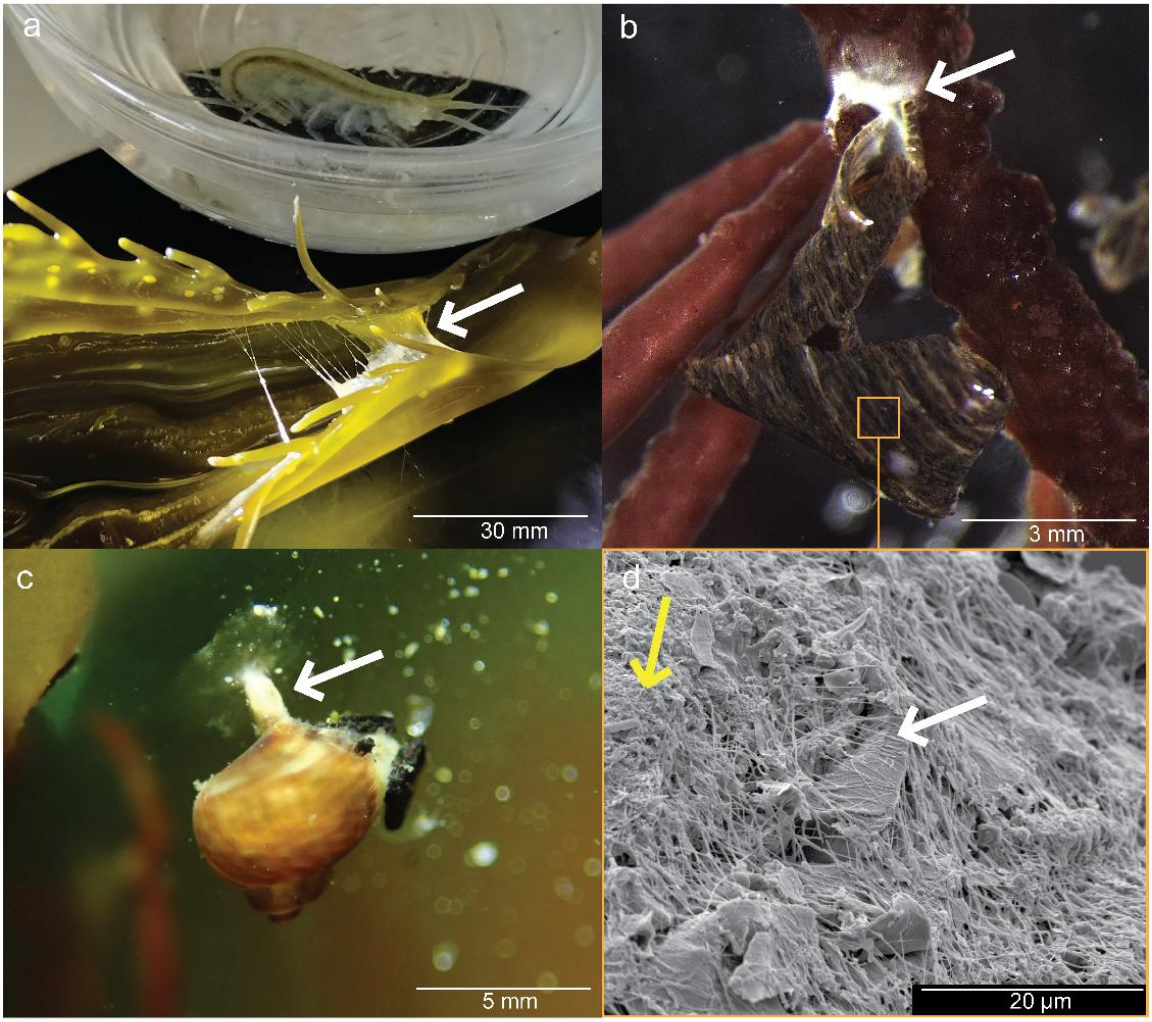


Fig. 1 Silk and silk structures from corophiidan amphipods. White arrows indicate attachment silk in a-c. **a** *Sunamphitoe humeralis* Stimpson, 1864 (Ampithoidae) attachment silk, used to stitch together folded kelp blades in half. Kelp blade partially opened here to remove the live female amphipod (visible behind). **b** *Notopoma sp.* A silk tube (brown) sliced open, with white attachment silk binding tube to red algae. **c** *Photis conchicola* Alderman, 1936 (Photidae) domicile inside of an old snail shell, with attachment silk binding the domicile to green algae. **d** SEM close up of *Notopoma sp*. A tube made of silk threads (white arrow), and amorphous silk (yellow arrow).

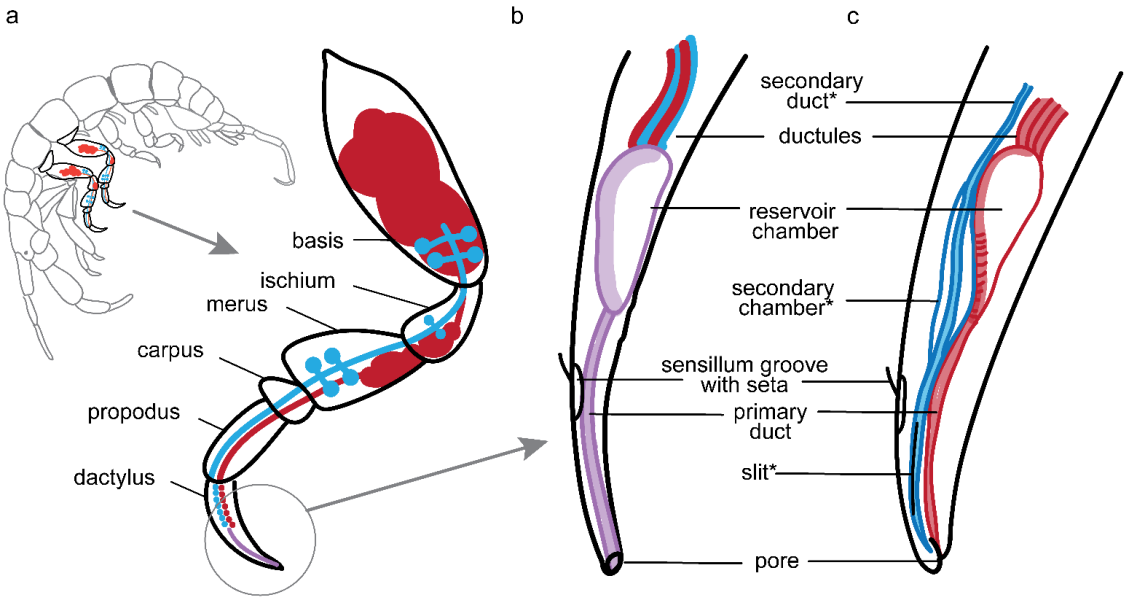


Fig. 2 Illustrations of silk-spinning pereopods and dactylus tips of corophiidans. **a** Generalized pereopods 3 and 4 showing the proximal gland (red), distal gland (blue); names of articles are shown. **b** Generalized historical representation of the dactylus tip of silk-spinning pereopods with products from both glands mixing (purple) in the reservoir chamber. **c** Generalized representation of our updated dactylus tip of silk-spinning pereopods that depicts two systems, the primary system (red) and the second system (blue). The primary system is associated with the proximal gland (red), and the second system is associated with the distal gland (blue). Asterisks indicate morphological characters identified in this present study not previously characterized.

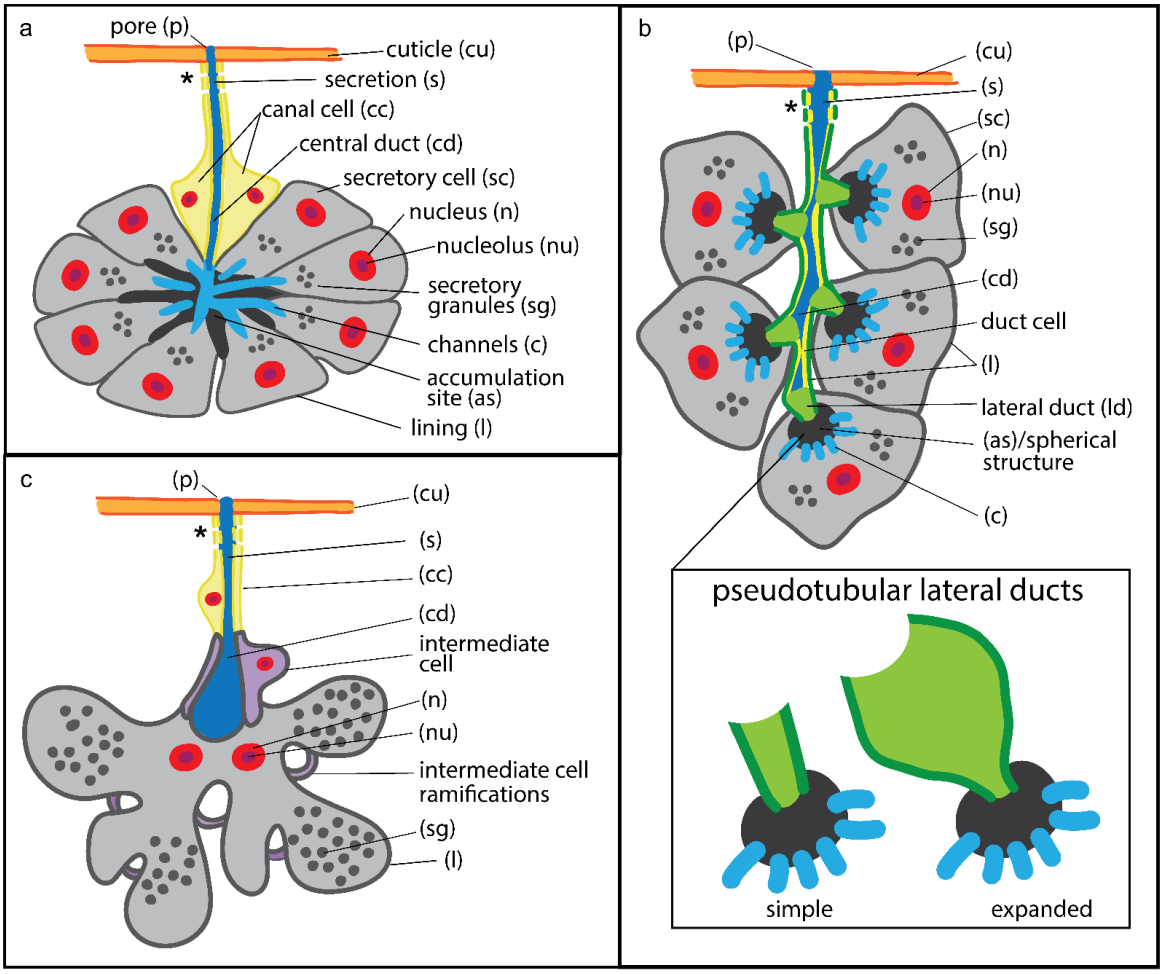


Fig. 3 Illustrations of exocrine gland types found in Peracarida crustaceans and their characteristics; adapted from Neretin *et al.* (2017) and Talbot & Demers (1993). Asterisks indicate areas where length is reduced. **a** Rosette gland, found in Tanaidacea but also described in corophiidans in Kronenberger *et al*. (2012a). **b** Pseudotubular gland described in corophiidans in Neretin *et al*. (2017) and in this present study. Inset is a close up of the two types of lateral ducts found in corophiidans: simple and expanded. **c** Lobed gland, found in Isopoda (Gorvett, 1952) and Tanaidacea (Kakui & Hiruta, 2014) but also described in corophiidans in Kronenberger *et al.* (2012a).

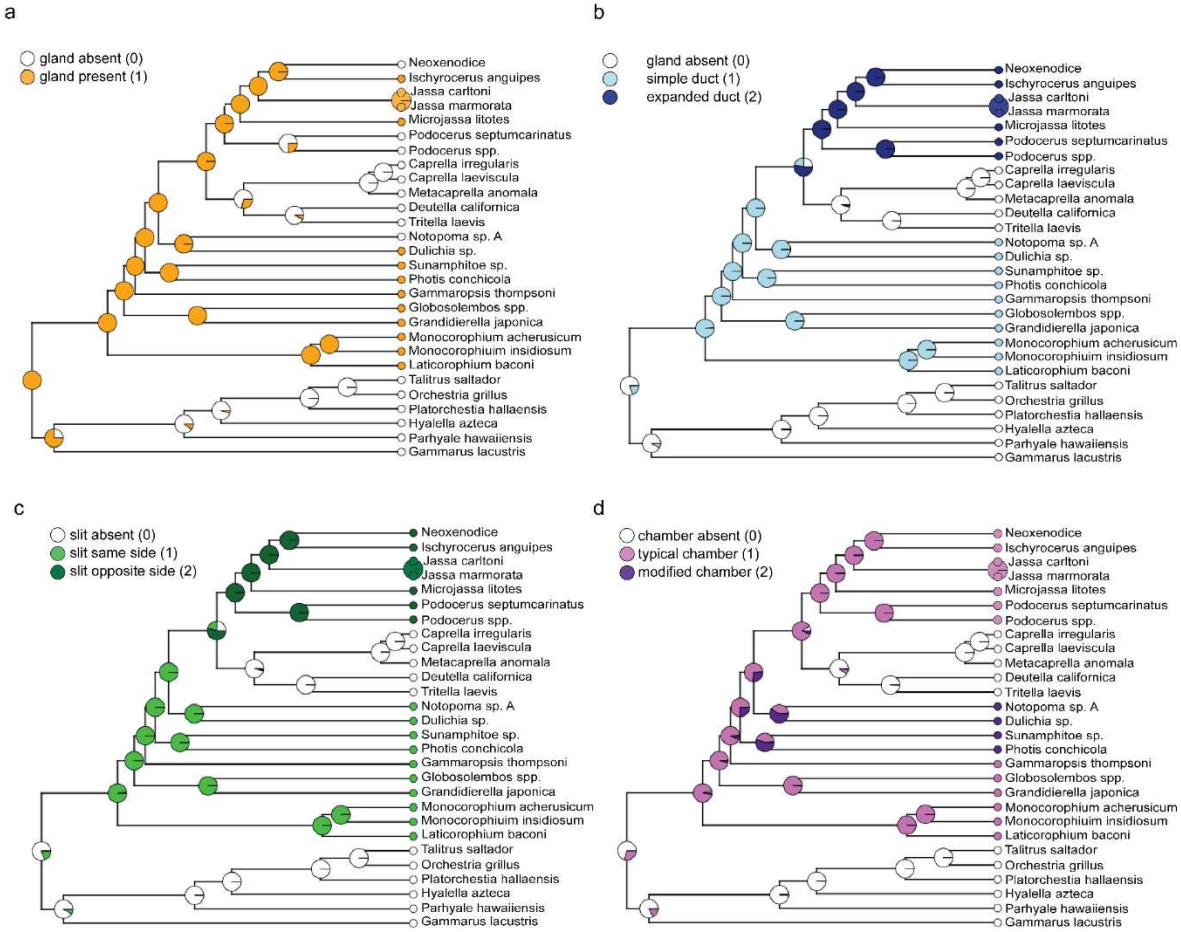


Fig. 4. Marginal ancestral state reconstruction analyses of four key silk-spinning characters in pereopods 3 and 4. Circles at the tips are observations of extant lineages and piegraphs at nodes are marginal probabilities of character states. **a** Proximal gland presence: present or absent. **b** Distal gland lateral duct type: absent, simple, or expanded. **c** Dactylus slit location in relation to the seta sensillum groove: absent, slit same side, slit opposite site. **d** Reservoir chamber type: absent, typical chamber, modified chamber. Colors of character states also correspond to states in Fig. 9.

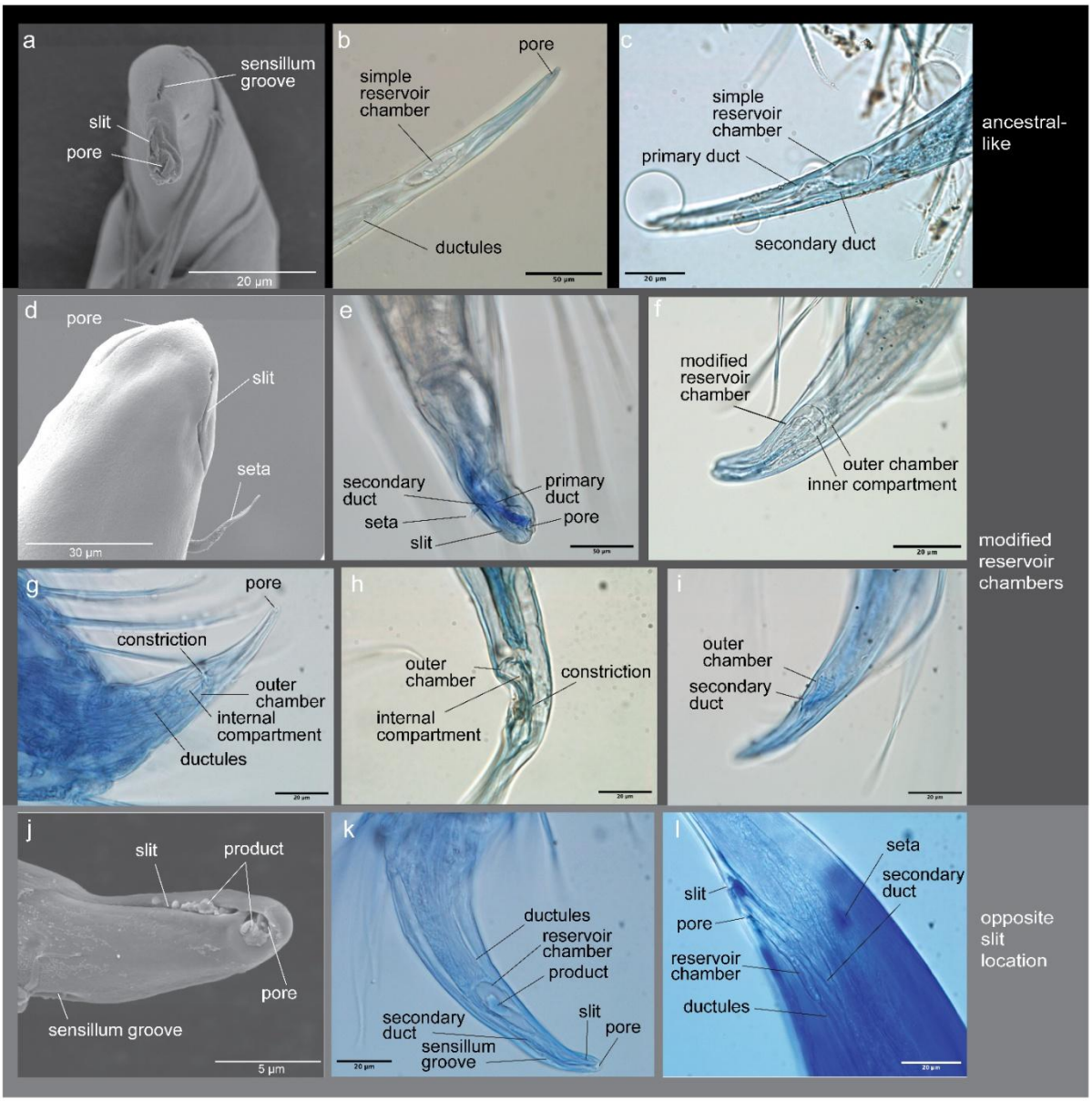


Fig. 5. Silk-extrusion morphology in pereopod 3 or 4 dactylus of corophiidans amphipods, labeled with key characters. a, d, & j are SEM images and b, c, e, f, g, h, i, k, & l are light microscope images of bromophenol blue stained dactyli. **a** *Aoroides secundus* left pereopod 4. **b** *Grandidireilla japonica* Stephensen, 1938 right pereopod 4 z-projection image. **c** *Monocorophium acherusicum* right pereopod 3. **d** *Sunamphitoe humeralis* right pereopod 3. **e** *S. humeralis* right pereopod 3. **f** *Ampithoe valida* right pereopod 3. **f** *Notopoma sp.* A left pereopod 3. **h** *Dyopedos monocanthus* right pereopod 4. **i** *Photis lacia* Barnard, 1962 right pereopod 3. **j** *Jassa carltoni* Conlan, 1990 left pereopod 4. **k** *J. carltoni* left pereopod 3. **l** *Podocerus cristatus* Thomson, 1879 right pereopod 3.

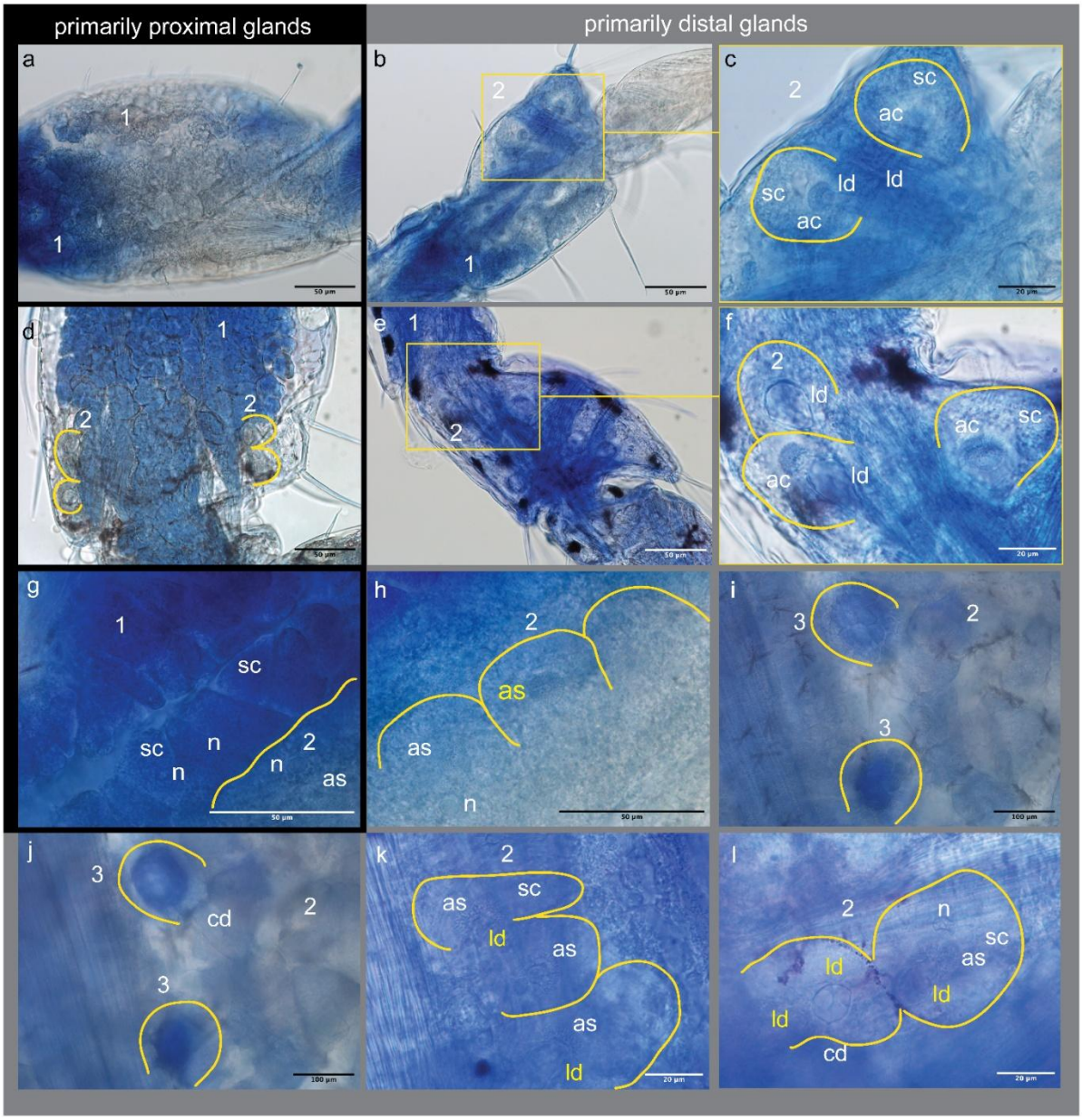


Fig. 6. Silk-spinning glands of corophiidan amphipods pereopods 3 or 4, stained with bromophenol blue. Yellow lines outline parts of glands. Yellow letters are characters of interest. Legend system same as Fig. 3; Legend: 1 = proximal gland, 2 = distal gland, 3 = different gland type in Ampithoidae, as = accumulation site, sc = secretory cell, ld = lateral duct, cd = central duct, n = nucleus. **a** *Americorophium stimpsoni* right pereopod 4 basis. **b** *A. stimpsoni* right pereopod 4 ischium, carpus, merus with square around distal merus. **c** *A. stimpsoni* right pereopod 4 close up of distal merus with simple distal gland. **d** *Ishcyrocerus anguipes* Krøyer, 1838 right pereopod 3 distal basis and proximal ischium. **e** *Jassa carltoni* right pereopod 3 ischium, merus, and carpus with square around ischium and proximal merus. **f** *J. carltoni* right pereopod 3 close up of distal ischium and proximal merus, highlighting distal gland with expanded lateral ducts. **g** *Ampithoe valida* right pereopod 4 basis ventral. **h** *A. valida* right pereopod 4 basis middle. **i** *Sunamphitoe humeralis* right pereopod 4 basis with third gland type. **j** *S. humeralis* right pereopod 4 basis with third gland. Same area as i but different focus plane. **k** *Podocerus cristatus* left pereopod 4 propodus with distal gland. **l** *P. cristatus* left pereopod 4 carpus with distal gland.

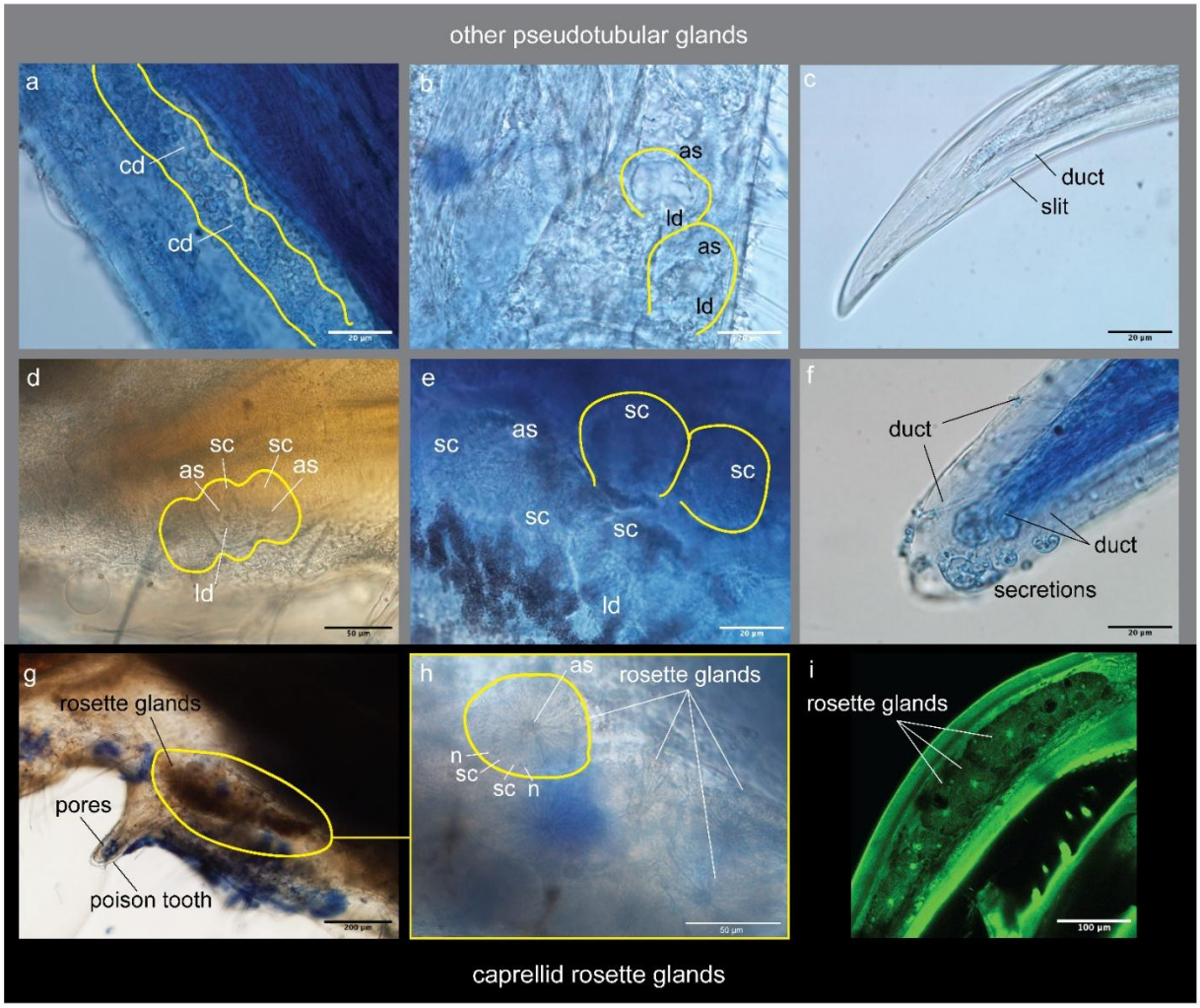


Fig. 7. Pereopodal glands in non-silk-spinning pereopods of corophiidan amphipods. Yellow lines outline glands in a, g, h, & i and secretory cells of gland in b-e. a-h bromophenol blue stained and light microscope imaged. i no stain and confocal image. Legend: as = accumulation site, sc = secretory cell, ld = lateral duct, cd = central duct, n = nucleus. **a** *Neoxenodice sp*. RP5 basis glands. **b** *Neoxenodice sp*. Right pereopod 5 merus glands. **c** *Neoxenodice sp*. right pereopod 4 dactylus. **d** *Neoxenodice sp*. right pereopod 2 propodus palm gland. **e** *Ericthonius rubricornis* male left pereopod 2 propodus palm gland. **f** *Jassa marmorata* male left pereopod 2 propodus thumb with secretory pores. **g** *Caprella mutica* Schurin, 1935 male right pereopod 2 propodus palm with rosette glands and poison tooth. **h** *C. mutica* right pereopod 2 close up of image g. **i** *C. mutica* female left pereopod 2 dactylus with rosette glands.

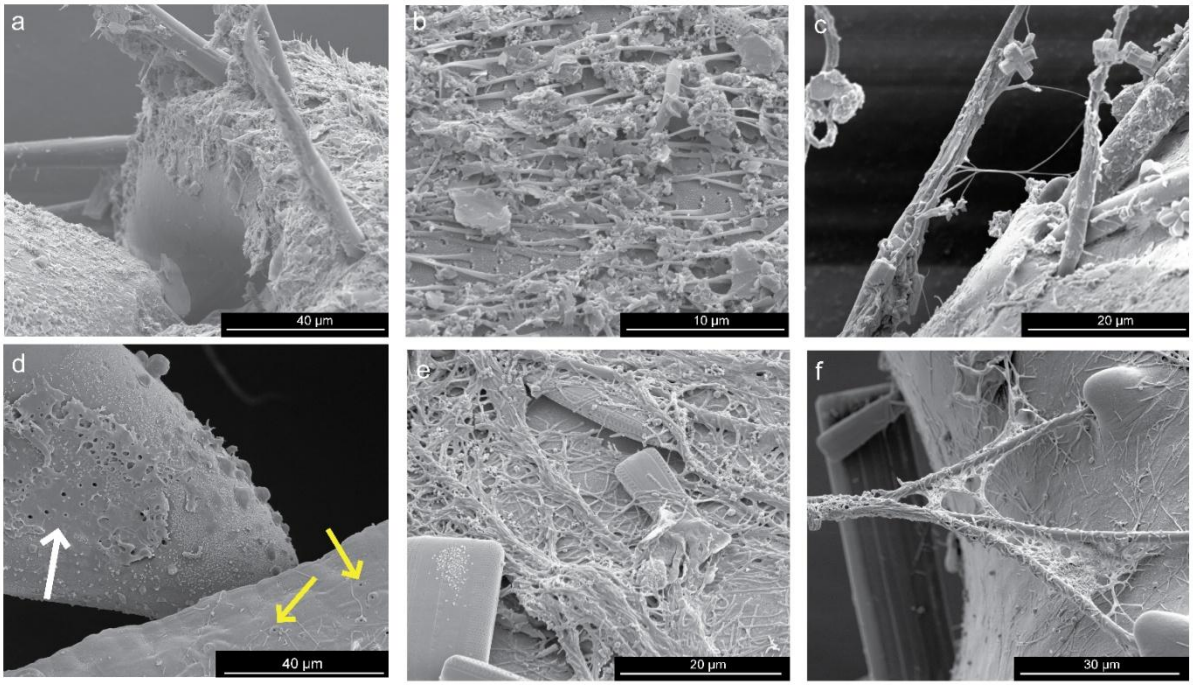


Fig. 8. SEM photos of corophiidan pereopod external morphology. **a** *Podocerus cristatus* pereopod 4 covered in secretions and detritus. **b** Close up of *P. cristatus* pereopod 4 with threads secretions from cuticle pores and detritus. **c** SEM of *P. brasiliensis* Dana, 1853 pereopod 4 threads on setae. **d** *Caprella mutica* male pereopod 2 poison tooth with pores and secretions (white arrow) and dactylus pores (yellow arrow) secreting threads. **e** Close up of *C. mutica* male pereopod 2 dactylus covered in threads and diatoms. **f** *C. mutica* male pereopod 2 palm setae covered in threads and cuticle pores visible.

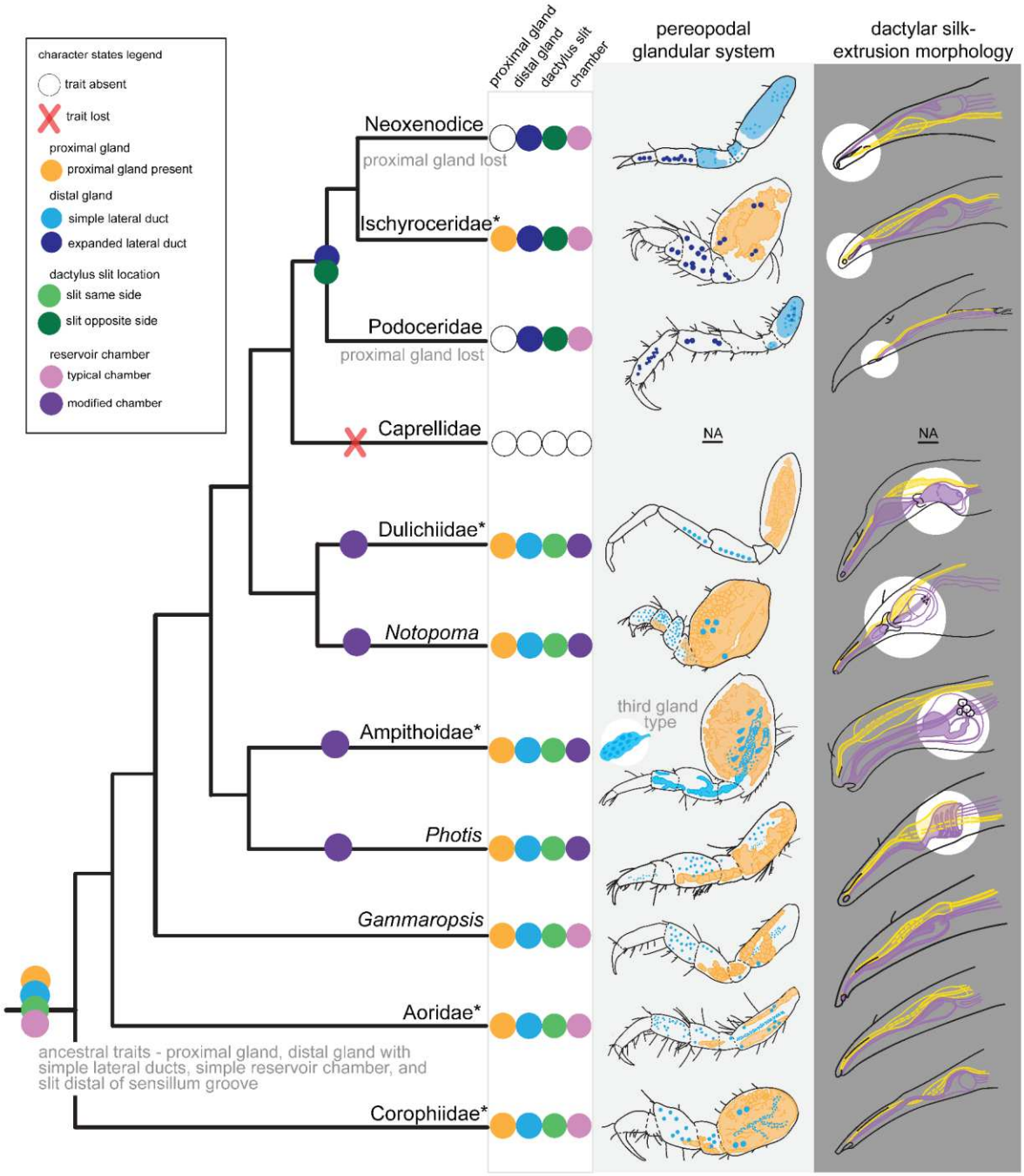


Fig. 9. The diversity and evolution of silk-spinning pereopods in corophiidans based on ancestral state reconstruction analyses with illustrations of pereopods and dactylus tips based on examined specimens. Lineages reduced to family or genus. Lineages with an asterisk have had their glandular morphology examined in previous literature. Illustrations in the pereopodal glandular system column: proximal gland (orange), distal gland with simple (light blue) and expanded (dark blue) lateral ducts; ducts not depicted. Illustrations in the dactylus silk-extrusion morphology column: primary system (purple): ductules, primary chamber, and primary exit. Secondary system (yellow): secondary duct, secondary chamber, and slit. White circles highlight modified chambers and translocated dactylus slits.

Supplementary Files

This is a list of supplementary files associated with this preprint. Click to download.

- SupplementaryInformation.docx